Journal of Physics D: Applied Physics

LETTER

Influence of asymmetric surface screening conditions on vortex switching in a ferroelectric nanodot

To cite this article: P C Xiong *et al* 2021 *J. Phys. D: Appl. Phys.* **54** 28LT01

Letters

IOP Publishing

Journal of Physics D: Applied Physics

J. Phys. D: Appl. Phys. **54** (2021) 28LT01 (7pp)

https://doi.org/10.1088/1361-6463/abf863

Letter

Influence of asymmetric surface screening conditions on vortex switching in a ferroelectric nanodot

P C Xiong[1], S Yuan[2,*], Y L Liu[1] and B Wang[3,*]

[1] School of Aeronautics and Astronautics, Sun Yat-sen University, Guangzhou 510275, People's Republic of China
[2] School of Materials Science and Engineering, Harbin Institute of Technology, Shenzhen 518055, People's Republic of China
[3] Sino-French Institute of Nuclear Engineering and Technology, Sun Yat-sen University, Zhuhai 519082, People's Republic of China

E-mail: yuanshuai2019@hit.edu.cn and wangbiao@mail.sysu.edu.cn

Received 25 January 2021, revised 8 April 2021
Accepted for publication 15 April 2021
Published 4 May 2021

Abstract

The behaviors of vortex switching in a ferroelectric nanodot on different surface screening conditions are investigated by phase-field simulations. It is found that asymmetric electrical boundary conditions have a significant effect on the formation of vortex domain structures and play a deterministic role in manipulating the vortex chirality by a homogeneous electrostatic field. The results indicate that the critical electric field for vortex switching can be greatly reduced by engineering the asymmetric surface screening conditions in a ferroelectric nanodot with a regular structure and uniform composition.

Keywords: asymmetric surface screening, vortex switching, chirality, phase-field model

(Some figures may appear in colour only in the online journal)

1. Introduction

Polar topology in low dimensional ferroelectric materials is currently a hot topic in materials science and condensed matter physics. The polarized vortex as a typical ferroelectric topological structure, has attracted increasing attention due to its potential applications for high-density non-volatile memories, sensors, actuators, etc [1–3]. The presence of vortex domain structures in low dimensional ferroelectric materials is closely related to the near-open-circuited (OC) electrical boundary conditions. Due to poor screening conditions, the bound charges near the surface cannot be compensated by the free charges, resulting in a considerable depolarization field. The depolarization field plays a decisive role in the formation of nanoscale ferroelectric vortex. In the presence of the depolarization field, the head-to-tail electric dipoles rotate to decrease the electrostatic energy of the system and evolve into a closed domain structure called vortex with definite handedness. As a topological order parameter representing the handedness characteristics, chirality is one of the basic properties of vortex domain structure [4]. Distinct from ferromagnetic vortex, ferroelectric vortex possesses only chirality but no polarity. It is of significance to investigate the switching behaviors of ferroelectric vortex chirality for its potential applications.

The ferroelectric vortex state is firstly predicted in nanodots, nanowires, and nanodisks through first principles based effective Hamiltonian calculations [5, 6]. Since then, progress has been made in experiment and theory on ferroelectric

* Authors to whom any correspondence should be addressed.

vortex. First, it is theoretically proven that near-open-circuit electrical boundary conditions are the decisive factor in the formation of vortexes in nanostructures [7]. Further studies showed that stress and strain also played an important role in the formation and stabilization of the vortex [8, 9]. Experimentally, the existence of ferroelectric vortex was determined in $Pb(Zr,Ti)O_3$ nanostructures by scanning probe microscopy [1, 10, 11]. Another milestone is the observation of ferroelectric vortex arrays reported in $PbTiO_3$-$SrTiO_3$ superlattice [12]. In recent years, due to the potential application on high-density information storage, the chirality reversal of ferroelectric vortex has been investigated in theoretical research. Researchers have found that the vortex chirality can be controlled with the application of the point charge or rotational electric field [13–15]. Thereafter, a series of schemes for breaking symmetry were proposed, e.g. by introducing non-central void defect [16], pinning effect of dislocation [17], asymmetric geometric structure [18], and compositional gradient materials [19], etc, in which the homogeneous electric field worked. Recently, tip bias sweeping has been reported to manipulate ferroelectric vortex chirality [20].

The chirality control of ferroelectric vortex can be realized by homogenous electrostatic field. Previous work mentioned above either breaks the symmetry of geometric structure or the symmetry of material composition to achieve this goal. How to control the vortex chirality by homogenous electrostatic field in samples with a regular structure and uniform composition has attracted considerable attention. In fact, in addition to geometry and composition, boundary conditions also play a significant role in the formation and stabilization of ferroelectric vortex. In previous work, almost all the studies on ferroelectric vortex domain structures were carried out under symmetrical electrical boundary conditions, including symmetric surface screening condition [21, 22]. So far, no research on the influence of asymmetric surface screening conditions on ferroelectric vortex has been reported. Due to the symmetry breaking by introducing different screening conditions onto different surfaces, it is feasible to investigate the reversal behavior of vortex chirality in a ferroelectric nanodot with regular geometry and uniform composition by using a homogeneous electric field.

2. Phase-field model

In this letter, we employ the phase-field model to study the influence of asymmetric surface screening conditions on the vortex chirality in ferroelectric nanodot. As part of the total polarization $\boldsymbol{P}^{\text{total}}$, the spontaneous polarization $\boldsymbol{P}$ is selected as the order parameter describing the ferroelectric domains. Thus, the electric displacement is expressed as $\boldsymbol{D} = \varepsilon_0\boldsymbol{E} + \boldsymbol{P}^{\text{total}} = \varepsilon_b\boldsymbol{E} + \boldsymbol{P}$, where $\boldsymbol{E}$ is electric field, ε_0 and ε_b are the vacuum dielectric constant and the background dielectric constant, respectively. According to the Landau–Ginzburg–Devonshire theory, the system-free energy is the sum of bulk Landau energy, gradient energy, elastic energy, electrostatic energy and surface energy, i.e. $F = \int_V (f_{\text{Land}} + f_{\text{grad}} + f_{\text{elas}} + f_{\text{elec}})\mathrm{d}V + \int_S f_{\text{surf}}\mathrm{d}S$, where f_{Land}, f_{grad}, f_{elas}, f_{elec} and f_{surf} represents the energy densities. For a ferroelectric system below Curie temperature, the specific expressions of these energy densities are as follows. For the bulk Landau energy density, $f_{\text{Land}} = a_{ij}P_iP_j + a_{ijkl}P_iP_jP_kP_l + a_{ijklmn}P_iP_jP_kP_lP_mP_n + a_{ijklmnop}P_iP_jP_kP_lP_mP_nP_oP_p$, where a_{ij}, a_{ijkl}, a_{ijklmn}, and $a_{ijklmnop}$ are the phenomenological coefficients which determine the thermodynamic behavior of the ferroelectric material. For the gradient energy density, $f_{\text{grad}} = \frac{1}{2}G_{ijkl}P_{i,j}P_{k,l}$, where G_{ijkl} is the gradient energy coefficient of spontaneous polarizations which deeply influences the formation and behavior of ferroelectric domain walls. For the elastic energy density, $f_{\text{elas}} = \frac{1}{2}C_{ijkl}\varepsilon^e_{ij}\varepsilon^e_{kl} = \frac{1}{2}C_{ijkl}(\varepsilon_{ij} - \varepsilon^0_{ij})(\varepsilon_{kl} - \varepsilon^0_{kl})$, where C_{ijkl} represent the stiffness coefficients which reflect deformation capacity of the material. ε_{ij}, ε^e_{ij} and ε^0_{ij} are the total strain, elastic strain, and eigenstrain tensor, respectively. For perovskite ferroelectrics, the eigenstrain is determined by spontaneous polarization, i.e. $\varepsilon^0_{ij} = Q_{ijkl}P_kP_l$, where Q_{ijkl} is the electrostrictive coefficients of the ferroelectrics. For the electrostatic energy density, $f_{\text{elec}} = -P_iE_i - \frac{1}{2}\varepsilon_bE_iE_i$. For surface energy density, $f_{\text{surf}} = \frac{1}{2}(\frac{D^S_1}{\delta^{\text{eff}}_1}P^2_1 + \frac{D^S_2}{\delta^{\text{eff}}_2}P^2_2 + \frac{D^S_3}{\delta^{\text{eff}}_3}P^2_3)$, where D^S_i is the surface coefficients related to the gradient energy coefficient and the surface normal vector, and δ^{eff}_i is the extrapolation length which measures the relaxation effect of eigenstrain near the surfaces. By integrating the above free energy densities over the entire volume and surfaces, the total Helmholtz free energy is achieved. The evolution of the spontaneous polarization field over time can be described by the variation of total free energy on polarization, which is expressed by the time-dependent Ginzburg-Landau equation, $\partial P_i/\partial t = -L\partial F/\partial P_i$, where L is the kinetic coefficient related to the domain wall mobility. The corresponding Newman boundary condition is $n_jG_{ijkl}P_{k,l} + \omega_{ij}P_j = 0$, where $\omega_{ij} = \text{diag}(D^s_1/\delta^{\text{eff}}_1, D^s_2/\delta^{\text{eff}}_2, D^s_3/\delta^{\text{eff}}_3)$ and n_i is the outward normal unit vector of a specific surface. Besides, the mechanical equilibrium equations are considered as $\sigma_{ij,j} = 0$, where the stress tensor $\sigma_{ij} = C_{ijkl}\varepsilon_{kl}$. Correspondingly, the Newman boundary condition is $n_j\sigma_{ij} = \tau_i$, in which τ_i represent the external loads. Meanwhile, the Maxwell equation, $D_{i,i} = -\varepsilon_b\varphi_{,ii} + P_{i,i} = 0$, is introduced to describe the electrostatic field distribution, where φ is the electric potential. Considering the surface charge screening effect, a screening factor θ that belongs to $[0, 1]$ is introduced to approximately express the surface charge screening level [23]. To be specific, the depolarization field is expressed as $(1-\theta)E^{\text{dep}}_i$. In other words, $\theta = 0$ refers to ideal OC electric boundary conditions in which the depolarization field reaches maximum, and $\theta = 1$ refers to ideal short-circuited conditions with the depolarization field vanishing. As θ increases from 0 to 1, the depolarization field gradually lowers in magnitude, and screening conditions change from open circuit to short circuit. In perovskite ferroelectrics, the above three sets of governing equations and boundary conditions can describe various evolution behaviors of domain structures.

In the following simulations, a freestanding $PbTiO_3$ (PTO) nanodot is chosen to study the effect of surface screening conditions on vortex chirality by a two-dimensional

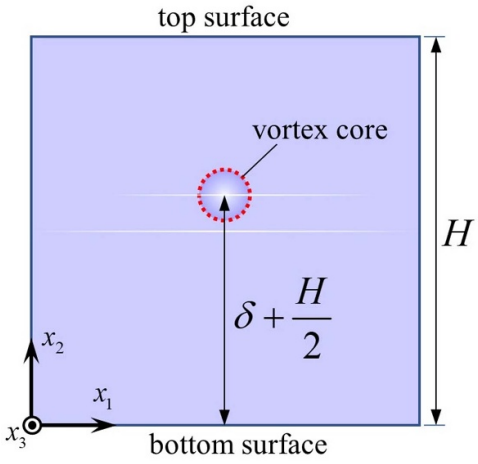

Figure 1. Schematic of a square ferroelectric nanodot with uniform composition. The side length of the nanodot is H, and the eccentric distance of the vortex core from neutral surface is δ.

(2D) phase-field model. A regular square nanodot with side length H is selected for investigation and the 2D Cartesian coordinates are established as depicted in figure 1. The mechanical boundary conditions on all surfaces are traction-free, that is $n_j\sigma_{ij} = 0$, thus the spontaneous strain generated by the electrostrictive effect can be fully relaxed in each direction. The electric boundary condition on the surfaces except the top one is open-circuited, i.e. $\theta = 0$ and $n_iD_i = 0$. Distinct from the bottom surface, the top surface satisfies charge screening condition, in which θ ranges from 0 to 1. In our simulation, we choose $H = 8$ nm and the room temperature $T = 300$ K as the default conditions. We mesh the nanodot into 20×20 elements, and select random polarization perturbation at each node according to the Gaussian distribution as the initial polarization condition. The values of all the parameters of PTO are taken from [24–29]. For the convenience of a numerical solution, all the parameters and variables in this work are nondimensionalized [30]. As the temperature decreases below the Curie temperature, a first-order phase transition from paraelectric to ferroelectric phase occurs in the nanodot. Under the OC boundary condition, the depolarization field near the surfaces gets the maximum due to the lack of compensation of free charges. As a result, the electric dipoles near the surfaces rotate to form a vortex with a head-to-tail arrangement to reduce the depolarization field to the greatest extent. Distinct from the ferromagnetic vortex, the ferroelectric vortex exerts a planar chiral domain structure wherein the polarization near the vortex core is zero. As seen in figure 1, we define the distance from the bottom surface to the vortex core as $\delta + H/2$, wherein δ represent the offset between the vortex core position with minimum polarization and the geometric central position of the specimen. In general, the ferroelectric vortex chirality can be characterized by the toroidilization $\boldsymbol{G}$, i.e. $\boldsymbol{G} = V^{-1}\int \boldsymbol{r} \times \left(\boldsymbol{P} - \bar{\boldsymbol{P}}\right)\mathrm{d}V$, in which $\boldsymbol{r}$ is position vector and $\bar{\boldsymbol{P}}$ is the average volume of the polarization [3]. Apparently, if $G > 0$, the vortex is counterclockwise (CCW), vice versa, the vortex is clockwise (CW).

3. Results and discussions

In previous work, the electrical boundary conditions in low dimensional ferroelectric materials are generally chosen to be symmetric, resulting in the vortex domain structure formed in a nanodot with regular geometry and uniform composition being symmetric. The chirality of an ideal symmetric vortex cannot be reversed by homogenous electrostatic electric field. Thus, different beneficial schemes have been proposed to generate an asymmetric vortex in a ferroelectric nanodot, e.g. by introduction of structure design or composition gradient. In fact, in addition to the geometric structure and composition, boundary conditions play a significant role in the forming process of vortex domain as well. Here, we consider the effect of asymmetric electrical boundary condition on the formation and transformation of ferroelectric vortex.

3.1. Effect of asymmetric surface screening on vortex domain structures

The schematic of electric boundary conditions in the nanodot is inserted in figure 2(b). Charge screening effect adjusted by θ is considered existent on the top surface. For other surfaces other than the top, OC boundary conditions are satisfied, i.e. $\theta = 0$. For $\theta \in (0, 1)$, the top surface is under incomplete screening condition due to partial compensation of free charge. Under the asymmetric electrical boundary conditions between the top and bottom surfaces, the ferroelectric vortex will be asymmetric along x_2-axis. The polarization distributions in the nanodot under different screening conditions, i.e. $\theta = 0,\ 0.8,\ 0.9,\ 1$, are depicted in figure 2(a). The white cones indicate the direction of the polarizations, and the color bar represents the magnitude of polarization, wherein the polarization $P = \sqrt{P_1^2 + P_2^2}$. Due to the top surface with ideal OC boundary condition when $\theta = 0$, the vortex is symmetric and the offset $\delta = 0$ inherently. As the screening factor θ increases, the bound charges of the top surface are gradually compensated by free charges from electrode or ambient, resulting in the depolarization field lowering correspondingly. As shown in figure 2(b), when θ is less than 0.8, the offset of vortex core caused by incomplete screening conditions increases only slightly, and the vortex core basically maintains a circular region. In other words, the symmetry of ferroelectric vortex remains at a high level. When θ continues to increase, the circular vortex core starts to deform into an elliptic one along the x_2-axis. Thus, the vortex core position with the minimum polarization sharply moves towards the top surface. When θ is more than 0.99, the bound charges on the top surface are nearly compensated completely, resulting in δ approaches $H/2$. Herein, the ferroelectric domain structure is no longer a vortex due to its non-closure characteristics at the top surface.

3.2. Effect of asymmetric surface screening on chirality reversal of a vortex

In a regular nanodot with uniform composition, the ferroelectric vortex exerts perfectly symmetric domain pattern

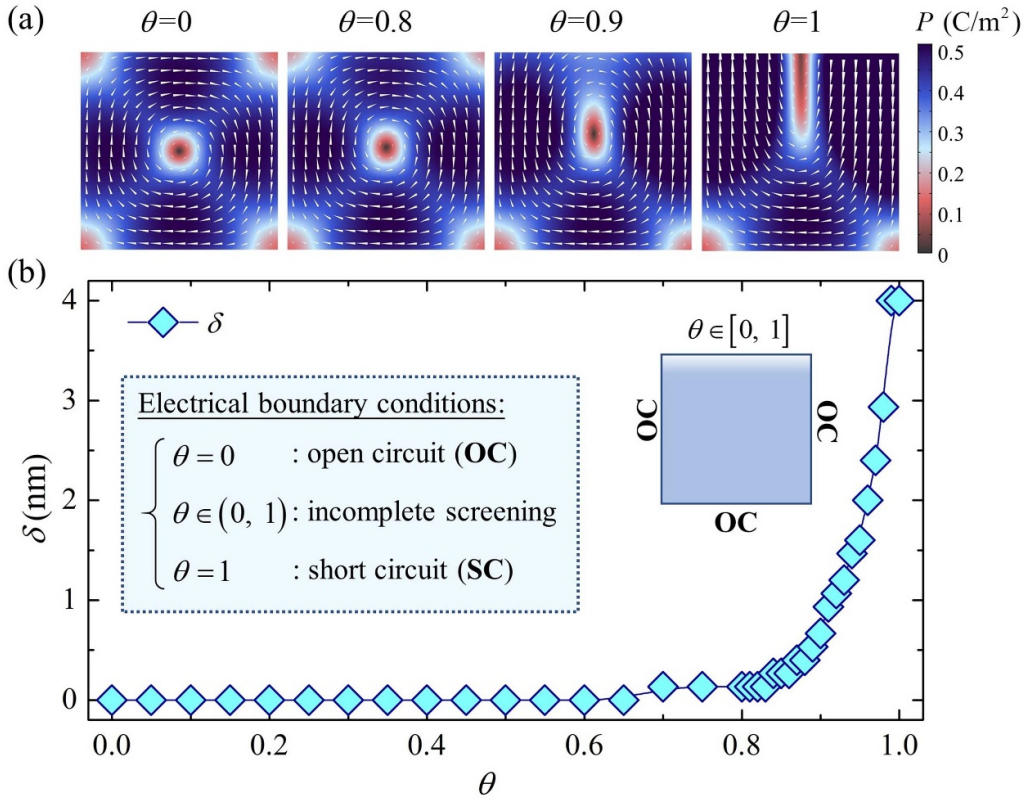

Figure 2. Influence of the top surface charge screening on the vortex domain structure in the nanodot. (a) Domain pattern for different screening factor $\theta = 0$, 0.8, 0.9, and 1. The color bar represents the magnitude of polarization. (b) Relation curve of screening factor θ and the offset δ. The schematic and illustration of electrical boundary conditions are inserted in (b).

resulting in no feasibility to manipulate its chirality by application of a homogeneous electric field. However, by introducing asymmetric electrical boundary conditions, it is made probable due to the symmetry of vortex domain structure being broken. Without loss of generality, we choose the case $\theta = 0.8$ to study the influence of the asymmetric screening effect on the reversal of vortex chirality. Under asymmetric surface screening conditions, the chirality of the vortex can be reversed by a uniform electrostatic field, which is loaded and unloaded according to the pattern in the inset in figure 3(b). The polarization evolution snapshots of the transformation from an initial CW vortex to a final CCW vortex are shown in figure 3(a). The transforming process is divided into three steps. In step I, for the dimensionless evolution time step $t^* = 0 \sim 100$, a CW vortex evolved from random polarization perturbation is selected as the initial state. In step II for $t^* = 100 \sim 200$, a homogenous electrostatic field is loaded and unloaded to the nanodot along the x_1-axis. In step III for $t^* = 200 \sim 300$, after the electric field is removed, the vortex chirality is reversed to CCW ultimately. The toroidilization evolution curve of the vortex switching is depicted in figure 3(b). Distinct from the color bar in figure 3(a) which represents the polarization magnitude, the color bar in figure 3(b) refers to the polarization orientation. As mentioned earlier, the offset δ of the vortex core is a very small value when $\theta = 0.8$, and the vortex is almost symmetric. In step I, the stable state A at $t^* = 80$ is an initial CW vortex state, and the toroidilization G in state A is -0.756 e Å^{-1}. In step II, with application of an external electric field $E = 2.9$ MV cm^{-1}, firstly the vortex core gradually moves along the negative direction of x_2-axis until it disappears at the bottom surface, afterwards, the nucleation and growth of a new vortex core occurs at the top surface due to the asymmetric screening condition. Typical states from B to G exhibit this transformation process. It is seen that the vortex domain structure experiences severe deformation during $t^* = 100 \sim 140$ after E loading, meanwhile the toroidilization changes from -0.688 e Å^{-1} in state B to 0.659 e Å^{-1} in state G. With the unloading of the external electric field, the new vortex core rapidly moves down along the negative direction of x_2-axis (state H $\sim$ I). As a result, a new vortex with a reverse chirality generates and stabilizes in step III. Stable state J at $t^* = 300$ is the final CCW vortex state in which the toroidilization is 0.756 e Å^{-1}. Ultimately, the CW vortex in a regular nanodot with uniform composition indeed be manipulated and reversed to the CCW vortex by external homogeneous electrostatic field.

Furthermore, the influence of different screening conditions on electrical switching of ferroelectric vortex at room temperature has been investigated. For different θ, the

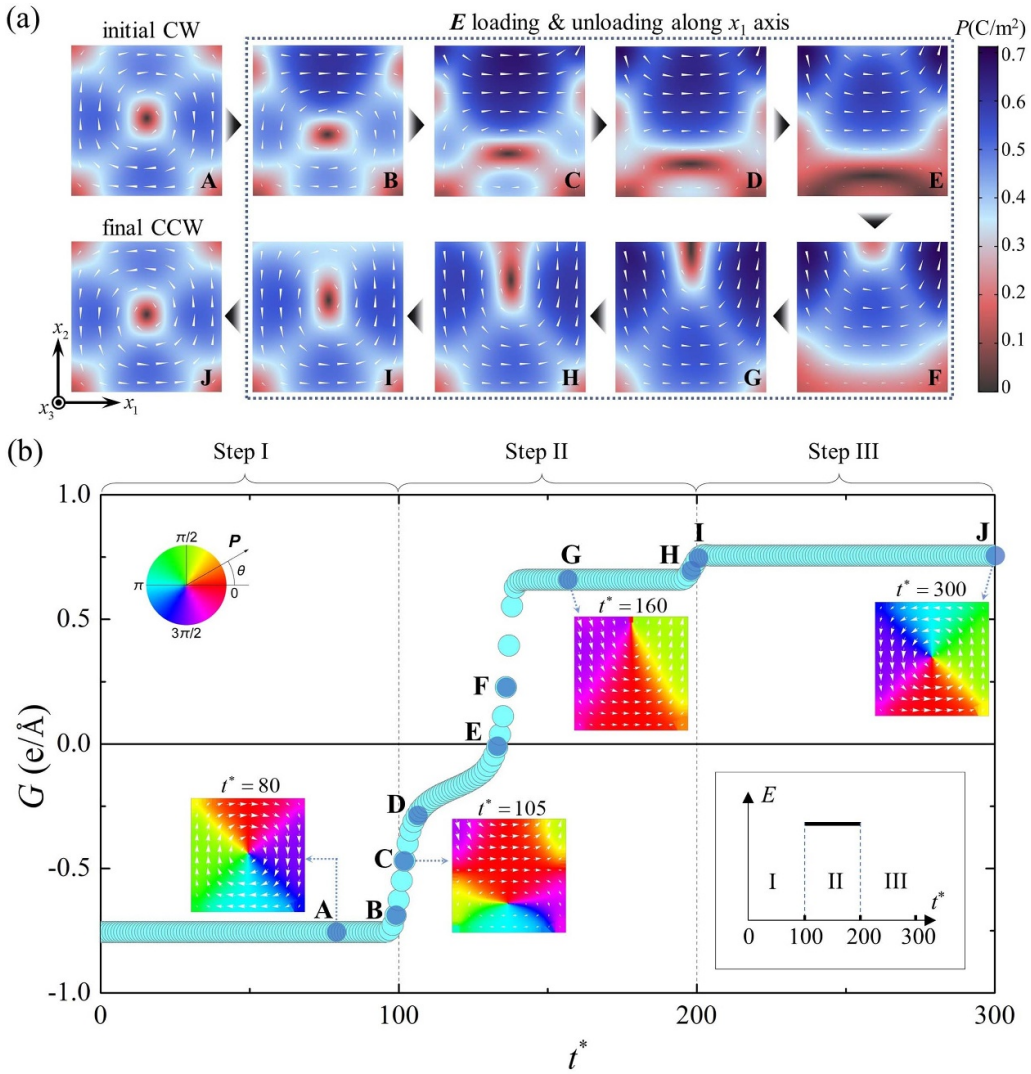

Figure 3. Vortex switching in the condition of $\theta = 0.8$ on the top surface of an 8 nm × 8 nm PTO nanodot by a homogeneous electrostatic field $E = 2.9$ MV cm^{-1} at room temperature. Three steps in the switching process: In step I, the initial vortex is clockwise (CW). In step II, the electric field E is loaded and unloaded along the x_1-axis. In step III, the final vortex is counterclockwise (CCW). (a) The evolution snapshots of vortex domain structures in step I ∼ III. The color bar represents the magnitude of polarization. (b) The evolution curve of vortex toroidilization G in the process of electrical switching. The color wheel represents the orientation of polarization. State A at $t^* = 80$ is chosen as an initial CW vortex in step I. States B ∼ I show the domain structures during E loading and unloading in step II. State J is the final CCW vortex after E unloading in step III. States A, G, and J are stable. The schematic of the electrostatic field loading is shown in the inset.

critical electric field for vortex switching is different. For the case of $\theta = 0$, and $\theta = 1$, the top surface satisfies OC and short-circuited boundary condition, respectively. There is no feasibility of vortex switching due to the vortex being perfect symmetric when $\theta = 0$. Meanwhile, the domain structure forming in the nanodot is no longer a closed vortex when $\theta = 1$, thus no vortex switching exists. Therefore, the typical cases of vortex switching for $\theta \in [0.05, 0.9]$ are considered to investigate the relationship between θ and the corresponding critical electric field E^c. As depicted in figure 4, it indicates that E^c decreases continuously with the increase of θ. When $\theta = 0.05$, E^c reaches 10.1 MV cm^{-1} owing to the symmetry of the vortex just being the slightly broken. Subsequently, the critical electric field drops sharply with the increase of θ. Finally, E^c decreases to 1.3 MV cm^{-1} in the case of $\theta = 0.9$. It can be revealed that the asymmetric surface screening effect plays a decisive role in the feasibility of ferroelectric vortex switching. Moreover, the greater the asymmetry of the electrical boundary conditions exerts, the easier the manipulation of vortex chirality by the homogenous electric field would be.

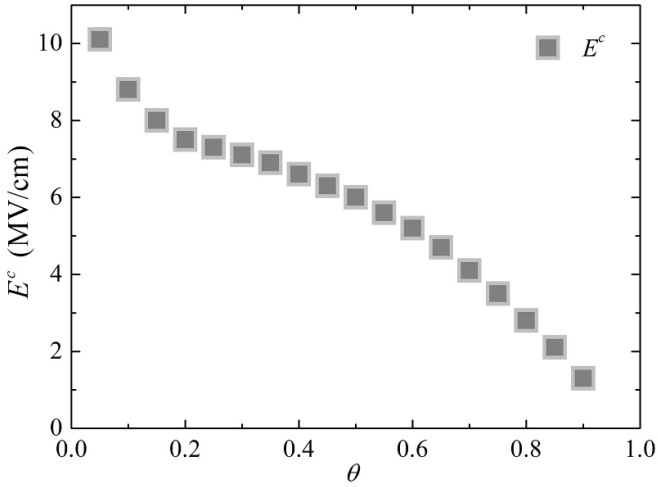

Figure 4. The relation curve of the critical electric field E^c for vortex switching and different screening factors on the top surface, wherein θ is taken from 0.05 to 0.90.

4. Conclusion

In summary, the influence of the asymmetric surface charge screening effect on the vortex state in a ferroelectric nanodot is investigated numerically based on phase-field simulation. Under the asymmetric surface screening effect, the vortex core is driven to deform and move to the surface with better screening conditions, which results in the symmetry-breaking of the vortex. It is this symmetry-breaking that is responsible for the electric switching of vortex chirality. The simulation results reveal the feasibility of the manipulation of the chirality of the ferroelectric vortex in a nanodot with a regular structure and uniform composition by application of a homogeneous electrostatic field. In fact, ferroelectric vortex domain structure is influenced significantly by boundary conditions, geometric structure, and material composition. Therefore, by satisfying appropriate electrical, mechanical or polarization boundary conditions, an asymmetric vortex can be obtained, and the vortex switching by homogenous electric field can also be achieved.

Data availability statement

The data that support the findings of this study are available upon reasonable request from the authors.

Funding

The authors gratefully acknowledge the financial support from China Postdoctoral Science Foundation (No. DB24407028), the Nature Science Foundation of China (Grant Nos. 11832019, 11472313, 13572355, 11572355), and Guangxi Science and Technology Program (Grant No. AD20159059). S Y also thanks the computing support from TianHe-2 of LvLiang Cloud Computing Center of China.

Conflict of interest

The authors declare no conflicts of interest.

ORCID iD

S Yuan https://orcid.org/0000-0002-4026-6597

References

[1] Gruverman A, Wu D, Fan H J, Vrejoiu I, Alexe M, Harrison R J and Scott J F 2008 Vortex ferroelectric domains *J. Phys.: Condens. Matter* **20** 342201
[2] Chen S Q *et al* 2021 Recent progress on topological structures in ferroic thin films and heterostructures *Adv. Mater.* **33** 2000857
[3] Zheng Y and Chen W J 2017 Characteristics and controllability of vortices in ferromagnetics, ferroelectrics, and multiferroics *Rep. Prog. Phys.* **80** 086501
[4] Shafer P *et al* 2018 Emergent chirality in the electric polarization texture of titanate superlattices *Proc. Natl Acad. Sci. USA* **115** 915
[5] Fu H and Bellaiche L 2003 Ferroelectricity in barium titanate quantum dots and wires *Phys. Rev. Lett.* **91** 257601
[6] Naumov I I, Bellaiche L and Fu H 2004 Unusual phase transitions in ferroelectric nanodisks and nanorods *Nature* **432** 737
[7] Prosandee S and Bellaiche L 2007 Characteristics and signatures of dipole vortices in ferroelectric nanodots: first-principles-based simulations and analytical expressions *Phys. Rev.* B **75** 094102
[8] Su Y and Du J N 2010 Effect of intrinsic surface stress on single-vertex structure of polarization in ferroelectric nanoparticles *Appl. Phys. Lett.* **96** 162905
[9] Shimada T, Wang X, Kondo Y and Kitamura T 2012 Absence of ferroelectric critical size in ultrathin $PbTiO_3$ nanotubes: a density-functional theory study *Phys. Rev. Lett.* **108** 067601
[10] Rodriguez B J, Gao X S, Liu L F, Lee W, Naumov I I, Bratkovsky A M, Hesse D and Alexe M 2009 Vortex polarization states in nanoscale ferroelectric arrays *Nano Lett.* **9** 1127
[11] Jia C L, Urban K W, Alexe M, Hesse D and Vrejoiu I 2011 Direct observation of continuous electric dipole rotation in flux-closure domains in ferroelectric $Pb(Zr,Ti)O_3$ *Science* **331** 1420
[12] Yadav A K *et al* 2016 Observation of polar vortices in oxide superlattices *Nature* **530** 198
[13] Prosandeev S, Ponomareva I, Kornev I, Naumov I and Bellaiche L 2006 Controlling toroidal moment by means of an inhomogeneous static field: an *ab initio* study *Phys. Rev. Lett.* **96** 237601
[14] Naumov I I and Fu H X 2008 Cooperative response of $Pb(ZrTi)O_3$ nanoparticles to curled electric fields *Phys. Rev. Lett.* **101** 197601
[15] Wang J 2010 Switching mechanism of polarization vortex in single-crystal ferroelectric nanodots *Appl. Phys. Lett.* **97** 192901
[16] Prosandeev S, Ponomareva I, Kornev I and Bellaiche L 2008 Control of vortices by homogeneous fields in asymmetric ferroelectric and ferromagnetic rings *Phys. Rev. Lett.* **100** 047201
[17] Chen W J and Zheng Y 2015 Vortex switching in ferroelectric nanodots and its feasibility by a homogeneous electric field: effects of substrate, dislocations and local clamping force *Acta Mater.* **88** 41
[18] Lich L V, Shimada T, Wang J, Dinh V-H, Bui T Q and Kitamura T 2017 Switching the chirality of a ferroelectric

vortex in designed nanostructures by a homogeneous electric field *Phys. Rev.* B **96** 134119
[19] Lich L V, Le M-T, Bui T Q, Nguyen T-T, Shimada T, Kitamura T, Nguyen T-G and Dinh V-H 2019 Asymmetric flux-closure domains in compositionally graded nanoscale ferroelectrics and unusual switching of toroidal ordering by an irrotational electric field *Acta Mater.* **179** 215
[20] Ma L L, Ji Y, Chen W J, Liu J Y, Liu Y L, Wang B and Zheng Y 2018 Direct electrical switching of ferroelectric vortices by a sweeping biased tip *Acta Mater.* **158** 23
[21] Ji Y, Chen W J and Zheng Y 2019 Crossover of polar and toroidal orders in ferroelectric nanodots with a morphotropic phase boundary and nonvolatile polar-vortex transformations *Phys. Rev.* B **100** 014101
[22] Wu C M, Chen W J, Ma D C, Woo C H and Zheng Y 2012 Effects of the surface charge screening and temperature on the vortex domain patterns of ferroelectric nanodots *J. Appl. Phys.* **112** 104108
[23] Lai B-K, Ponomareva I, Naumov I I, Kornev I, Fu H X, Bellaiche L and Salamo G J 2006 Electric-field-induced domain evolution in ferroelectric ultrathin films *Phys. Rev. Lett.* **96** 137602
[24] Yuan S, Chen W J, Liu J Y, Liu Y L, Wang B and Zheng Y 2018 Torsion-induced vortex switching and skyrmion-like state in ferroelectric nanodisks *J. Phys.-Condes. Matter* **30** 465304
[25] Pertsev N A, Zembilgotov A G and Tagantsev A K 1998 Effect of mechanical boundary conditions on phase diagrams of epitaxial ferroelectric thin films *Phys. Rev. Lett.* **80** 1988
[26] Wang J J, Ma X Q, Li Q, Britson J and Chen L Q 2013 Phase transitions and domain structures of ferroelectric nanoparticles: phase field model incorporating strong elastic and dielectric inhomogeneity *Acta Mater.* **61** 7591
[27] Zheng Y and Woo C H 2009 Thermodynamic modeling of critical properties of ferroelectric superlattices in nano-scale *Appl. Phys.* A **97** 617
[28] Woo C H and Zheng Y 2008 Depolarization in modeling nano-scale ferroelectrics using the Landau free energy functional *Appl. Phys.* A **91** 59
[29] Ishikawa K and Uemori T 1999 Surface relaxation in ferroelectric perovskites *Phys. Rev.* B **60** 11841
[30] Yuan S, Chen W J, Ma L L, Ji Y, Xiong W M, Liu J Y, Liu Y L, Wang B and Zheng Y 2018 Defect-mediated vortex multiplication and annihilation in ferroelectrics and the feasibility of vortex switching by stress *Acta Mater.* **148** 330